



# Effect of wind, river discharge, and outer-shelf phenomena on circulation dynamics of the Atchafalaya Bay and shelf



Mohammad Nabi Allahdadi<sup>b</sup>, Felix Jose<sup>a,\*</sup>, Eurico J. D'Sa<sup>b</sup>, Dong S. Ko<sup>c</sup>

<sup>a</sup> Department of Marine & Ecological Sciences, Florida Gulf Coast University, Fort Myers, FL, USA

<sup>b</sup> Louisiana State University, Department of Oceanography and Coastal Sciences, Coastal Studies Institute, Baton Rouge, LA, USA

<sup>c</sup> Oceanography Division, Naval Research Laboratory, Stennis Space Center, MS, USA

## ARTICLE INFO

### Keywords:

Atchafalaya Bay  
Mike 3 model  
Coastal currents  
Lagrangian model  
Vertical eddy viscosity  
Cold fronts

## ABSTRACT

The influence of wind, river discharge, and outer-shelf variations on the circulation of the Atchafalaya Bay and the adjoining inner shelf were examined using a 3-dimensional circulation model. Current and water level data from three stations along a transect off the Marsh Island were used for model calibration and skill assessment. Coastal current and its spatial distribution were significantly affected by open boundary conditions. Model sensitivity analysis suggested that the vertical eddy viscosity has a substantial impact on the energy and momentum transfer across the water column in this shallow bay-shelf environment. It was also shown that westward to northwestward currents dominated in the study area during the non-summer months and that would transport westward large volume of sediments discharged from rivers during the spring flood season. This sediment load is contributing to the progradation of the Chenier Plain along the southwestern Louisiana coast. A particle tracking Lagrangian model validates the westward migration of suspended sediments originating from the river mouth area during the spring season.

## 1. Introduction

The Atchafalaya Bay, located on the western flank of Louisiana inner shelf, forms part of the greater Mississippi River drainage system. The Bay and the adjoining shelf are strongly influenced by the sheer volume of fresh water and sediment plume discharged from rivers, particularly during the spring flood season with circulation in the shallow shelf mainly driven by the wind (Allahdadi et al., 2011). About 19–29% of the river water and 30–40% of sediment load from the Mississippi River is diverted through the Atchafalaya River to the Atchafalaya-Vermillion Bay and then to the Gulf of Mexico (Mossa and Roberts, 1990; Allison et al., 2000; Walker and Hammack, 2000). Fresh water and sediment load are discharged through two main outlets, viz., Wax Lake outlet and Morgan City channel (Roberts and Sneider, 2000). For the inner Atchafalaya shelf, water quality is highly affected by seasonal hydrodynamics and morphology of the shelf, which modulates the salinity in the shelf and along the shoreline (Cobb et al., 2008a; Allahdadi et al., 2011). In this context, understanding the hydrodynamics within the Atchafalaya Bay and the adjoining inner shelf is essential for studies aiming to determine the fate and dispersal of fresh water and sediment load from the Atchafalaya

River. For instance, strong southward currents associated with passage of cold fronts during winter/spring season have been identified for their significant effect on sediment transport inside and outside of the Atchafalaya Bay (Feng and Li, 2010).

Currents in the Atchafalaya shelf follow the general circulation pattern of Louisiana coast (Cochrane and Kelley, 1986) and is influenced by seasonal wind, tides, river discharge, and outer-shelf variations induced by the Loop Current Eddies (Oey, 1995; Allahdadi et al., 2011). However, depending on the location, relative contribution of each individual forcing on the circulation is different and difficult to differentiate. A modeling study for the Louisiana shelf by Oey (1995) concluded that wind forcing accounts for up to 50% of the transport over the inner shelf with river discharge and outer shelf eddies contributing to the rest. Tide-generated currents are very weak due to the small tidal range over the Louisiana shelf (average of 0.4 m) and are of mixed-diurnal in nature (Wright et al., 1997). The dominant wind effect with varying direction for different seasons results in different circulation patterns. Easterly to south-easterly winds during most of the year (September to May) produce mostly westward (down-coast) currents over the inner-shelf (Cochrane and Kelly, 1986; Li et al., 1997; Allahdadi et al., 2013). A simultaneous eastward current produced by anticyclonic Loop Current eddies along the shelf break can generate a cyclonic gyre

\* Corresponding author.

circulation within the broad inner-shelf with a sustained down-coast current (Cochrane and Kelley, 1986). A shift in the wind direction to southwest during the summer produces a persistent, albeit weak, eastward current over the inner-shelf. At a shorter time scale, the frequent passage of cold fronts from late September to May, generates episodic offshore directed shelf currents (Rego, 2008; Cobb et al., 2008b; Feng and Li, 2010). Based on the analysis of met-ocean data from different bays along the Louisiana coast, Feng and Li (2010) observed that during the passage of cold fronts, northerly wind would generate strong southward (offshore directed) currents that could flush out about 40% of bay waters over a short period of time. This flushing can substantially modulate sediment transport characteristics and their depositional pattern over the Atchafalaya shelf (D'Sa et al., 2011; Tehrani et al., 2013).

Although several studies have already addressed wave dynamics and its interaction with the muddy bed of the Atchafalaya Bay and shelf (Siadatmousavi et al., 2012, 2013; Sheremet and Stone, 2003; Sheremet et al., 2005; Allison et al., 2000), a detailed study of shelf hydrodynamics and coastal current regime has been lacking. Cobb et al. (2008a, 2008b) used a northern Gulf of Mexico model to investigate the effect of cold fronts on salinity distribution and to some extent the circulation of the Atchafalaya Bay. They reported that during the pre-frontal phase, westward currents were amplified which could contribute to the transport of river sediments to the Chenier plains. The westward currents could also be modulated by river plume deflection as a result of the Coriolis effect (Kourafalou et al., 1996). Although that comprehensive study addressed some aspects of circulation over the inner Atchafalaya shelf, the focus was on the fate of fresh water discharged from the river. The present study uses a 3-dimensional hydrodynamic model implemented on a high-resolution flexible mesh to address the hydrodynamics of the extended Atchafalaya Bay-shelf system while also assessing the impact of different forcing and their sensitivity on the circulation. One key aspect of this study is to simulate the dispersal pathways of freshwater and sediment plumes coming out of the rivers during the peak flood season and to show how they are influenced by the prevailing wind and remote outer-shelf forcing. Outcome of this study can provide a proper base to evaluate the seasonal contribution of sediment load originating from the Atchafalaya River towards the buildup of Chenier coastline farther west of the study area.

Another objective of this study is to statistically quantify the relative contribution of different forcing (local as well as remote) in the shelf circulation. Although wind has been identified as the main forcing in driving the currents in the region (e.g., Allahdadi et al., 2011), the effect of outer-shelf variations in modulating the current field has not been thoroughly determined. A study of the hydrodynamics of the narrow eastern Louisiana shelf using outputs from a northern Gulf of Mexico model nested in a regional Intra-Americas Sea model (IASNFS; Ko et al., 2003; Ko and Wang, 2014) appropriately resolved the Loop Current eddies and their interaction with the currents on the Louisiana Shelf (Chaichitehrani et al., 2014). That study demonstrated the modulating effect of deep water eddies on the coastal currents in the vicinity of the Birds-Foot Delta and the adjoining shelf west of the delta. The present study attempts to numerically evaluate similar effects for the broad Atchafalaya bay/shelf region.

## 2. Study area and approach

The focus of the present study is the Atchafalaya Bay and the adjoining shelf (Fig. 1). Marsh Island, located along the southern fringe of the bay, is a rapidly eroding low lying barrier island that protects the northern bay (Vermillion Bay) from the open Gulf of Mexico. The shallow coastal zone is strongly impacted by the discharge from the

Atchafalaya River system, which brings high amounts of mud (consolidated and partially settled) that accumulates on the shelf (Sheremet and Stone, 2003; Jose et al., 2014; Siadatmousavi et al., 2012).

## 3. Model specifications

### 3.1. Numerical model

The 3-D hydrodynamics model, Mike3 FLOW MODEL-FM, developed by DHI water and Environment (DHI, 2014) was utilized to simulate the coastal currents and its spatial/temporal variability in response to wind, river discharge and tide/outer-shelf variations. The model solves Reynolds averaged Navier-Stokes and continuity equations based on a finite volume scheme on a domain composed of triangular elements on a horizontal plane.

For model discretization along the vertical direction, a finite difference approach using either  $z$  or  $\sigma$  coordinate or their combination is applied. Time varying 2-D wind data can be used for forcing the model with wind energy transferred through the water column via shear stress. There are different approaches for considering the effect of bottom friction on the current. Bottom friction parameter as well as the surface friction coefficient regulate the atmosphere-ocean coupling and can be fine-tuned for model calibration. A particle tracking tool based on a Lagrangian approach has been incorporated in Mike Zero module of the DHI software. This tool is used in this study for further analysis of simulated currents.

### 3.2. Model setup

#### 3.2.1. Data

**3.2.1.1. Bathymetry data.** Compared to the narrow shelf adjoining the Mississippi Bird-foot delta, the mid Louisiana shelf, especially the Atchafalaya shelf, is very wide with extensive shallow shoals off the Atchafalaya Bay (Fig. 1). Although the study area (Atchafalaya shelf and bay) encompasses only a smaller part of the Louisiana coast, a large modeling domain extending from the Mississippi Bird-foot delta to the western boundary of the Atchafalaya shelf was considered for simulating the effect of Louisiana coastal currents on the study area as well as accounting for the complex interaction of the shallow shelf with the outer continental shelf dynamics. Shelf-wide bathymetry data were obtained from NGDC (NOAA). Additionally, high resolution bathymetry survey data collected during 2008 from Tiger and Trinity Shoal Complex (Roberts et al., 2010) were used to refine the model grid for the shoal complex. Based on the available bathymetry data, the average depth within the Atchafalaya Bay is about 2.5 m. Water depth is 10 m at a distance of 35 km south of the bay entrance, while the 30 m isobath is located at a distance of ~70 km.

**3.2.1.2. NARR (NCEP) wind.** - NCEP North American Regional Re-analysis (NARR) wind data were extracted from the NCEP archives and used for the study. The NARR wind data with ~32 km spatial resolution has been extensively validated for the Gulf of Mexico (Jose and Stone 2006).

**3.2.1.3. NCOM/Navy Hydrodynamic data for boundary forcing.** The forcing from outside of the shallow Atchafalaya model domain could significantly affect the dynamics (e.g., current pattern) of the inner-shelf, especially along the eastern and southern boundaries. In order to take into account these far-field effects, boundary conditions along the open boundaries were extracted from archives of a coastal model based on NCOM (Navy Coastal Ocean Model). NCOM is a 3-D, free surface, primitive equations ocean model applying the hydrostatic, Boussinesq, and incompressible approximations (Martin, 2000; Barron et al.,

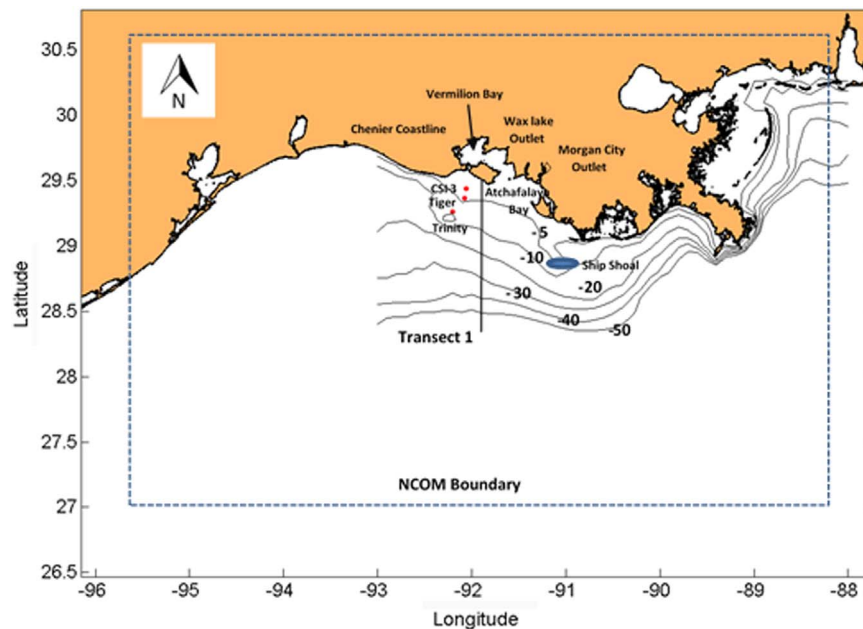


**Fig. 1.** Study area in the northern Gulf of Mexico showing locations of measurement stations in the Atchafalaya Bay/shelf (dots), transect1 discussed in the text (solid line), and boundaries of the NCOM model for the northern Gulf of Mexico (dashed rectangle). Contours are shown for 5, 10, 20, 30, 40, and 50 m of water depths over the Louisiana shelf.

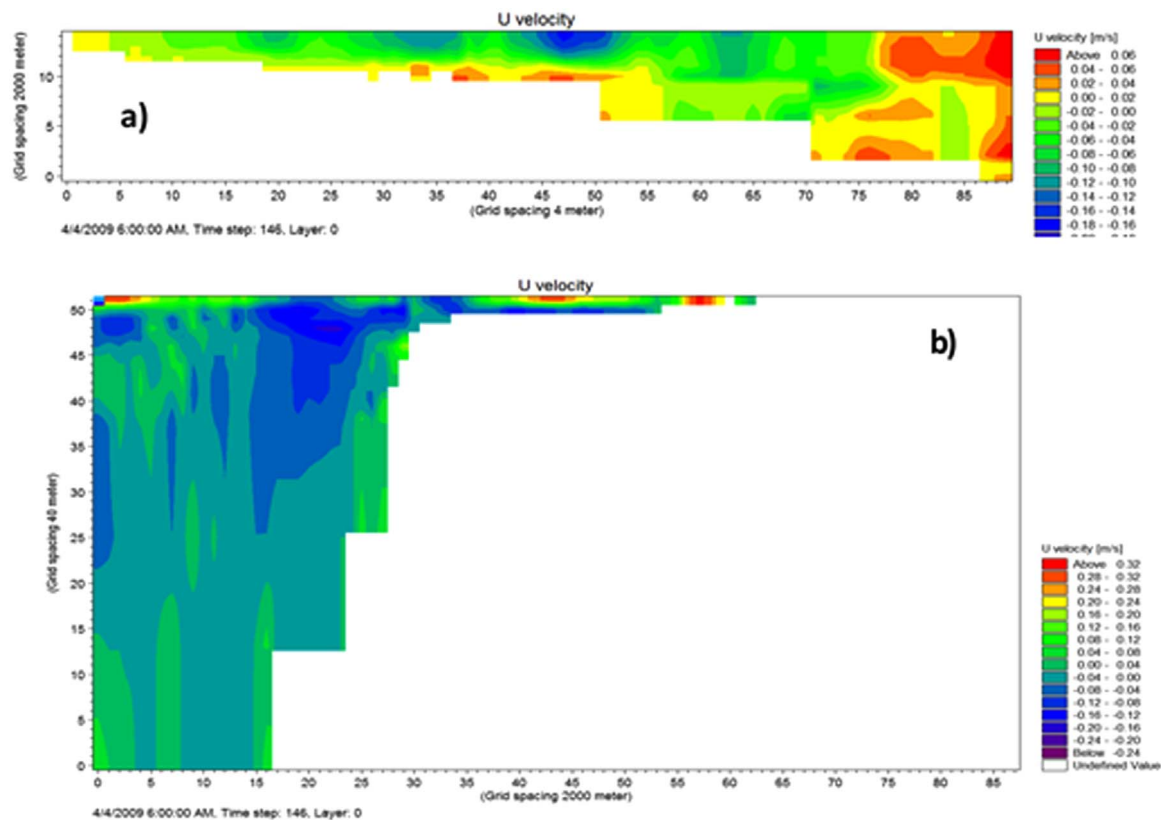


**Fig. 2.** Samples of extracted boundary conditions from the coastal model for u component of current along; a) the western boundary, b) the eastern boundary of the Atchafalaya model.

2006). Boundary conditions for the Atchafalaya shelf model were extracted from the coastal model comprising the Mississippi/Louisiana shelf and a part of eastern Texas shelf (model boundaries are shown with dashed rectangle in Fig. 1; D'Sa and Ko, 2008). This NCOM coastal model was itself nested within a regional NCOM ocean model, the IASNFS, which encompasses western North Atlantic, the Caribbean and the Gulf of Mexico and is forced with wind, air pressure, heat fluxes, and solar radiation from NOGAPS (Navy Operational

Global Atmospheric Prediction System) and assimilates the satellite altimeter data from MCSST. The nested NCOM coastal model properly simulated the Loop Current and its shedding off eddies with appropriate effect on the Louisiana shelf as indicated by the successful model application in assessing the particulate suspended matter and dissolved organic carbon dynamics over the Louisiana Shelf (D'Sa and Ko, 2008; Chaichitehrani et al., 2014). In this study, vertical profiles of currents were extracted for the western and eastern model

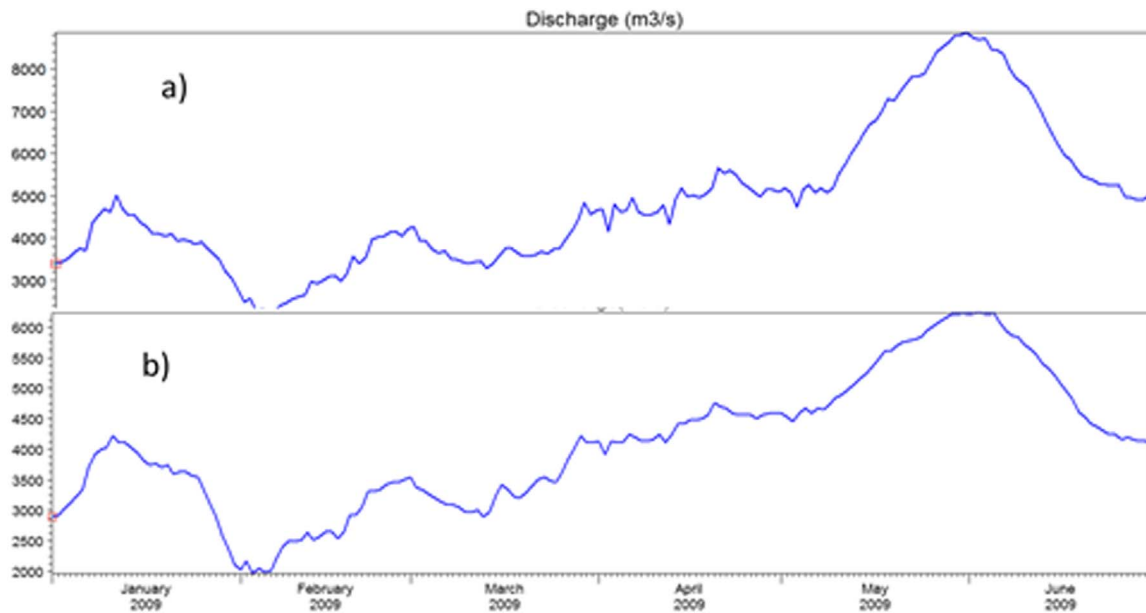


**Fig. 3.** Time series of Atchafalaya River discharge for six months in 2009 at; a) Morgan City station and b) Wax Lake station (Data courtesy, USGS).

boundaries (Fig. 2), while along the southern boundary, time-series of water level elevation data (including tide) were extracted for forcing the Atchafalaya model.

**3.2.1.4. Atchafalaya River discharge.** The study area near the Atchafalaya Delta is strongly influenced by fresh water discharge from the Atchafalaya River. Data on daily water discharge were used as input for the simulation. Two main discharge points of the Atchafalaya River are the Morgan City point in the eastern part of the Bay and the Wax Lake Outlet located in the middle of the Bay (see Fig. 1). River discharge data is available as daily averages obtained from USGS at each of these two locations (see Fig. 3).

**3.2.1.5. Field data on currents.** As the focus of this research is on the Atchafalaya shelf close to the bay entrance (Fig. 1), hydrodynamic data from two different sources inside the study area were used to examine the flow characteristics and for model calibration. One source was from an extensive field survey conducted along the Tiger and Trinity Shoal complex during March/April 2009 (Jose et al., 2014; Siadatmousavi et al., 2012, 2013). Hydrodynamic data from two stations along a transect that ran across the Tiger and Trinity Shoal complex (Fig. 1) were used for this study. The second set of data was from WAVCIS (WAVE-Current-surge Information System). WAVCIS is a monitoring system comprising of an array of met-ocean sensors on fixed offshore platforms located along the central Louisiana coast (Stone et al., 2009; Zhang, 2003) that provides hourly observations on directional waves, vertical current profiles, tide, wind speed and direction, air pressure, and sea surface temperature. These hourly data are transmitted via cellular communication to the WAVCIS Laboratory at Coastal Studies Institute, Louisiana State University ([www.wavcis.lsu.edu](http://www.wavcis.lsu.edu)). Teledyne RDI® Acoustic Doppler Current Profilers (ADCP) are used for wave and current measurements with vertical bin interval of 35–50 cm. Data used in this study was from station CSI-3 located at the mouth of Vermilion Bay in shallow depths (~ 4.5 m) and within the study area (see Fig. 1 for the location).

Time series of observed wind at CSI-3 and surface currents at three stations from the shoal complex between 18 March and 16 April 2009 (Fig. 4) showed persistent southeasterly winds prevailed during the

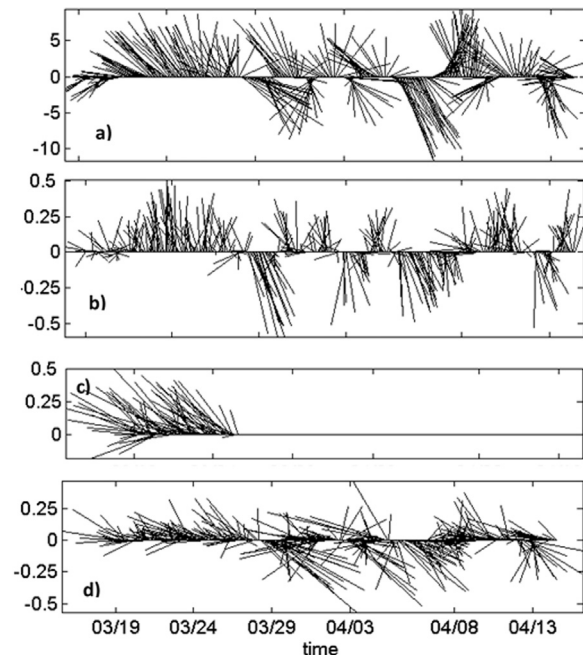


**Fig. 4.** Time series of measured a) wind at station CSI-3 and current speed at stations b) CSI-3, c) Tiger Shoal, and d) Trinity Shoal in March/April 2009 (wind and current speeds are in m/s).

first 10 days of the deployment with corresponding coastal currents being northward, northwestward, and westward at CSI-3, Tiger, and Trinity shoal stations, respectively. Cold front events from 29 March onwards (specifically on 29 March, 8 April, and 13 April when wind speed was up to 7–15 m/s) induced southward to southeastward currents at CSI-3 and Trinity locations (no data was available for Tiger station at this time) with maximum current speeds of 0.65 and 0.80 m/s, respectively. The currents turned northward after each frontal passage over the study area.

### 3.2.2. Computational mesh

A finite volume numerical scheme is used in Mike3-Flow FM model to solve the governing equations on a computational mesh which is made of triangular mesh elements on a horizontal plane. The triangular



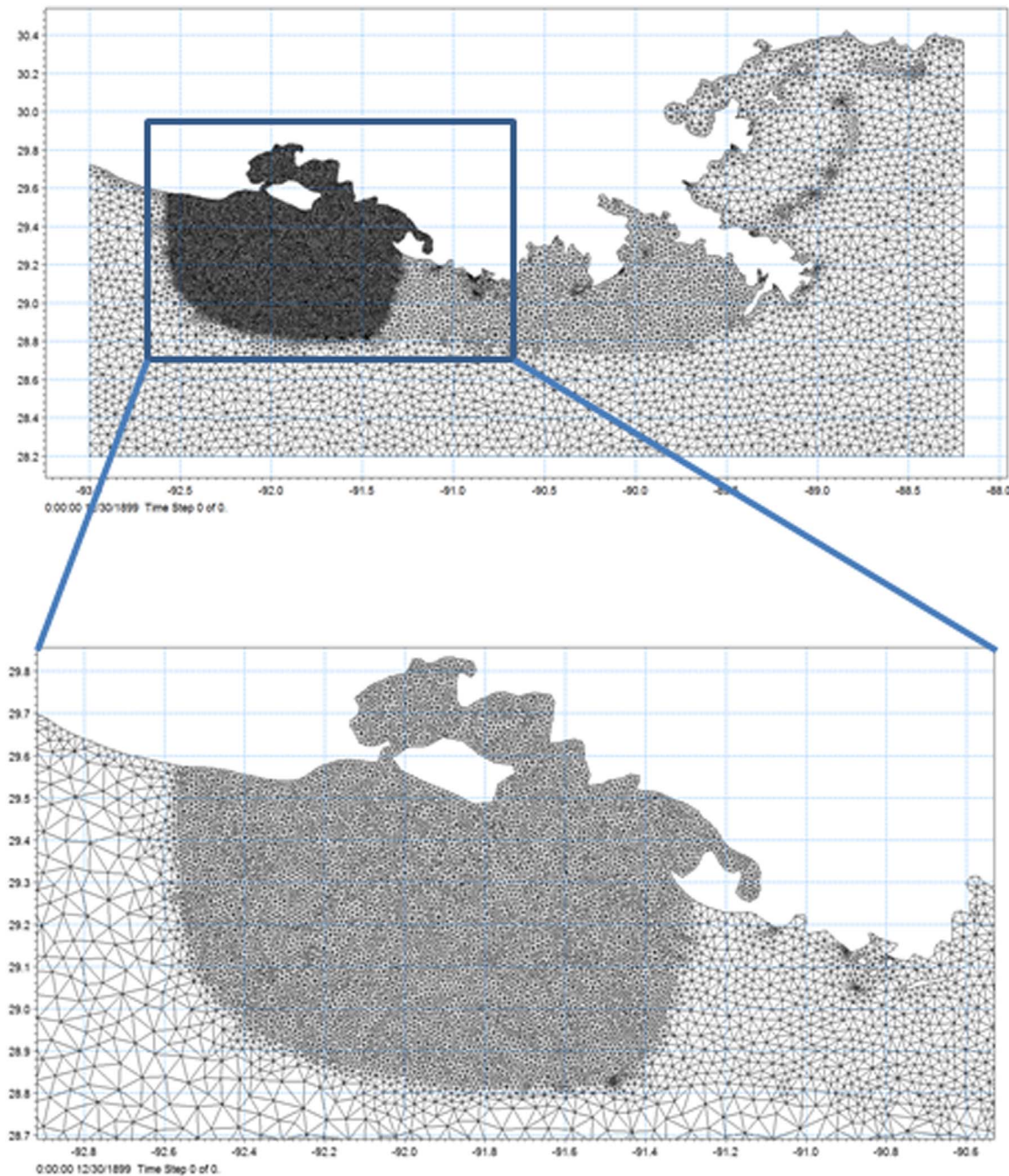


**Fig. 5.** The computational mesh (upper panel) and the zoomed-in view of the Atchafalaya Bay/shelf area.

flexible mesh offered high flexibility in grid generation so that a fine element mesh could be used when required within the model domain. As the emphasis was on Tiger and Trinity shoal area as well as the Atchafalaya Bay and adjacent shelf, a finer mesh was used for the shallow area with complex bathymetry, but slightly coarser for the shelf area to the east of Atchafalaya Bay and west of the Mississippi Bird-foot delta as this area can also have a significant effect on the coastal current pattern in the study area (Fig. 5).

#### 4. Numerical model implementation

The hydrodynamic model simulation was conducted for a one month period from 18 March to 16 April 2009, corresponding to the period when field data were available for the Tiger and Trinity shoal complex. Before using the simulation outputs for studying the hydro-

dynamics of the Atchafalaya shelf, sensitivity analysis was conducted to evaluate the relative importance of boundary forcing fields on the circulation dynamics of the region. Other modeling parameters including vertical eddy viscosity, bottom friction coefficient, and wind drag coefficient were tuned through model calibration using field data on coastal currents and water level.

##### 4.1. Model sensitivity for boundary forcing

Although wind is considered to be the main current driving force over the Louisiana shelf, the effect of tide and outer-shelf variations could be significant (Oey, 1995). As such we took boundary forcing from a high resolution northern Gulf of Mexico model (NCOM, see Section 3.2.1.c) for the Atchafalaya shelf model. The impact of this boundary condition on the circulation over the shallow shelf surround-

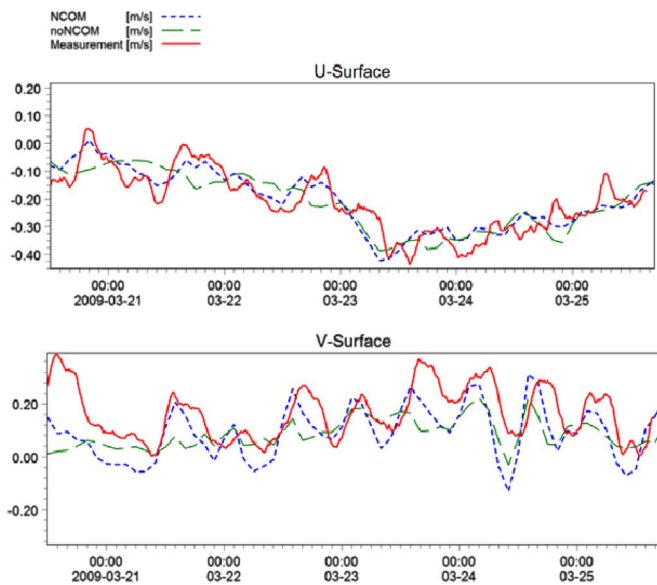


**Fig. 6.** Impact of boundary forcing on simulated surface currents at Tiger station. Upper panel: u current component; lower panel: v current component. Simulation case studies included using NCOM data as the boundary condition (NCOM) and skipping boundary data (no-NCOM).

ing the Atchafalaya Bay was examined by performing model simulations with and without boundary forcing from the coastal model. This analysis would assist for further quantifying the effect of current generating forces over the study area. Simulation results were compared with measured current and water level data within the model domain. For simulating both u and v current components, enabling boundary forcing from the coastal model appears to significantly improve the model outputs (Fig. 6; shown for velocity components at Tiger shoal station) especially during the peaks of the currents.

#### 4.2. Effect of vertical eddy viscosity ( $K_z$ )

Rate of vertical energy transfer, which is controlled by the vertical eddy viscosity ( $K_z$ ) within the water column can substantially affect velocity magnitudes and even circulation pattern (Csanady, 1972; Park and Kuo, 1996; Saenko, 2006; Zhang and Steele, 2007). Vertical eddy viscosity as the main calibration parameter was successfully used for simulating coastal current characteristics over the Louisiana shelf (Allahdadi et al., 2011). In order to investigate the impact of vertical eddy viscosity on simulated currents in the study area, model results from several simulations using different values of the  $K_z$ , ranging from 0.0001 to 2  $\text{m}^2/\text{s}$ , were examined. Results showed significant differences between the simulated currents based on the upper and lower bounds of the considered  $K_z$  range. Simulated currents using smaller  $K_z$  (0.004  $\text{m}^2/\text{s}$ ) exhibited better agreement with measurements as indicated by calibration data (Fig. 7).

#### 4.3. Model skill assessment

As part of the model skill assessment, simulated current velocities were compared with measured current and water level data. Model parameters were fine-tuned to obtain the best possible agreement. Sensitivity analysis provided in Sections 4.1 and 4.2 showed that including coastal model boundary forcing as well as using 0.004  $\text{m}^2/\text{s}$  for the vertical eddy viscosity provided the best agreement with measurements. Other calibration procedures including tuning the bottom friction coefficient and the drag coefficient for the wind forcing have been performed. Results (not shown) were not as significant as those changes for vertical eddy viscosity.

In the following model simulations a constant value of 0.001m was

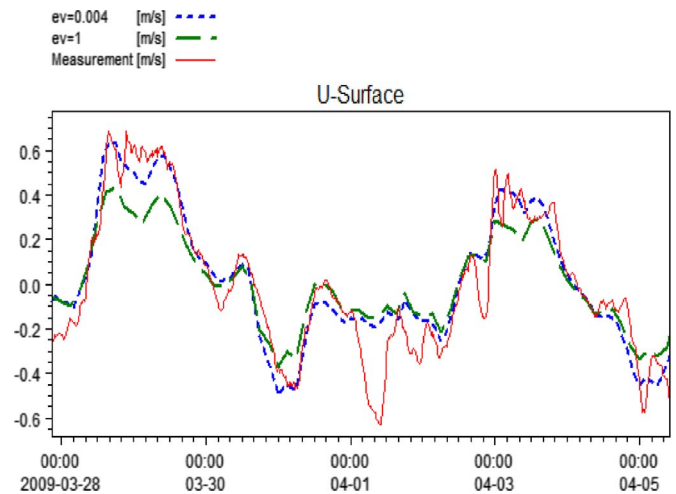


**Fig. 7.** Comparison of measured data with simulated u current values at Trinity station for different values of the vertical eddy viscosity.

used as the bed roughness height to compute bottom friction. Wind drag coefficient was considered 0.00125 for wind speeds smaller than 7 m/s and 0.00250 for wind speeds larger than 25 m/s. For wind speeds between 7 and 25 m/s a linear variation between two values was considered. The data from both Trinity shoal and CSI-3 were available for the entire one month modeling period (from mid-March to mid-April), while for the Tiger shoal location, measurements were available for a shorter period (19–27 March 2009), due to instrument malfunction (Jose et al., 2014). Comparison of measured and simulated u and v current components from all 3 stations (Figs. 8–10) and simulated water level data at Trinity shoal station (Fig. 9 lower panel) indicate good agreement between model and measurements for most of the cases. An index of agreement ( $d$ ) proposed by Willmott (1981) was used for quantification of model performance in the simulation of currents and water level. The index is represented as:

$$d = 1 - \frac{\sum_{j=1}^n [y(j) - x(j)]^2}{\sum_{j=1}^n [|y(j) - \bar{y}| + |x(j) - \bar{x}|]^2}$$

where,  $x(j)$  are measured values,  $y(j)$  are simulated values, and  $\bar{x}$  and  $\bar{y}$  represent the mean values of measurement and simulation, respectively. Index values vary between 0 for poor agreement and 1 for a perfect match. Table 1 shows the values of the index for all model validations shown in Figs. 8–10. For all cases the index value is larger than 0.6, with the highest  $d$  value, indicating the high accuracy of simulations, obtained for the deeper Trinity shoal location. The lower index values for simulated currents at the CSI3 and Tiger stations, compared to Trinity station, could be due to inaccuracies associated with uncertainty in the bottom frictional coefficient at these two stations in the simulations.

## 5. Model outputs

### 5.1. Current pattern

The calibrated model was employed to study the circulation dynamics of the study area, especially for the Tiger and Trinity shoal complex. Model outputs were evaluated for various wind conditions (Fig. 11) as the main current-inducing force in the area. Wind events were selected as discrete events considered within the 1-month modeling period as mentioned in Section 4. Simulated current and water level data (Fig. 12a) resulted from southeasterly wind with sustained speed of 10 m/s (Fig. 11a; extracted from NARR/NOAA archives for the Louisiana shelf) demonstrate the generation of north-westward currents as strong as 0.4 m/s over southeast of the

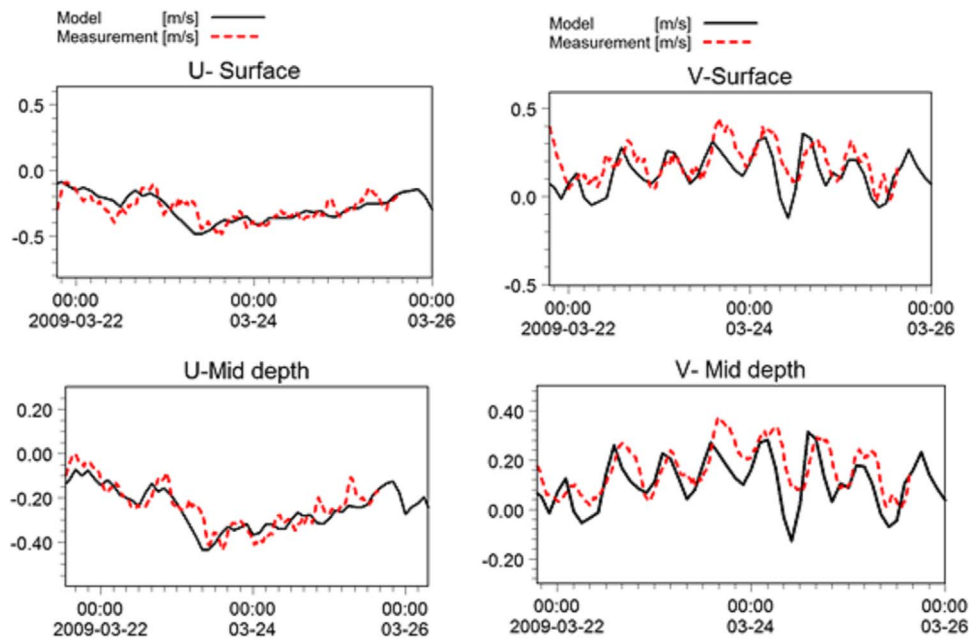


Fig. 8. Comparison of measured and simulated currents at Tiger shoal.

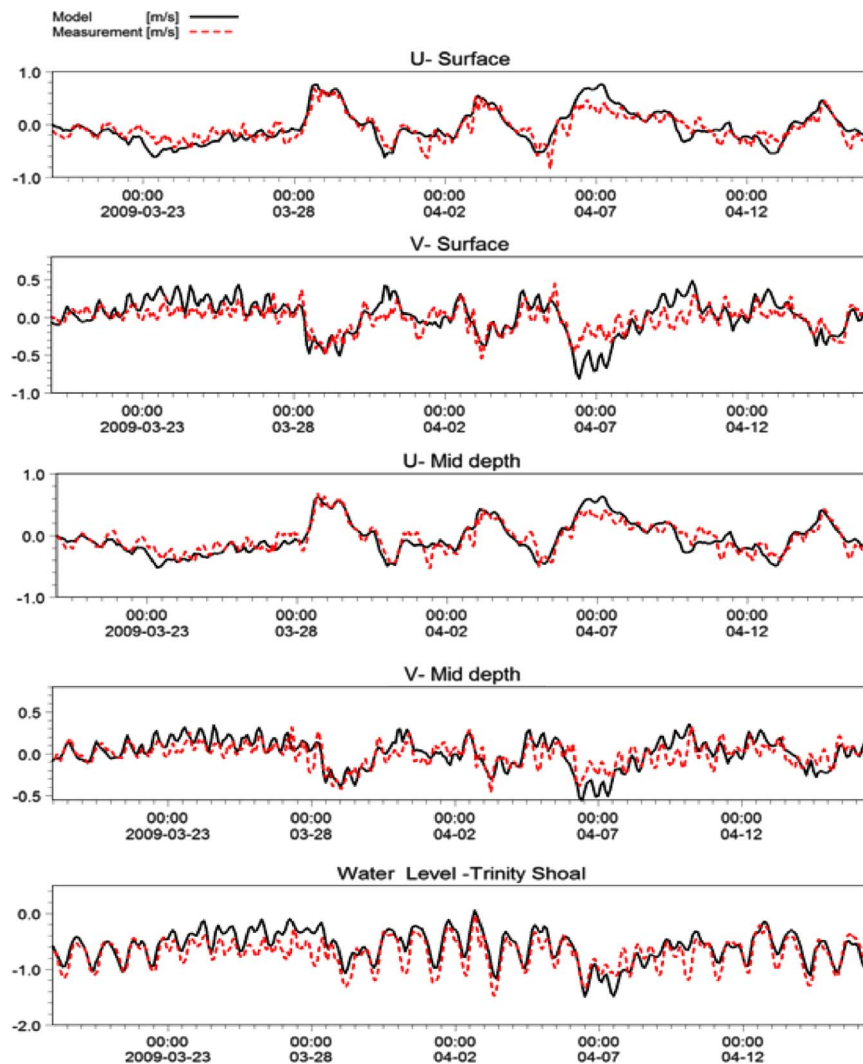


Fig. 9. Comparison of measured and simulated currents and water level for Trinity shoal. (water level is in meter).



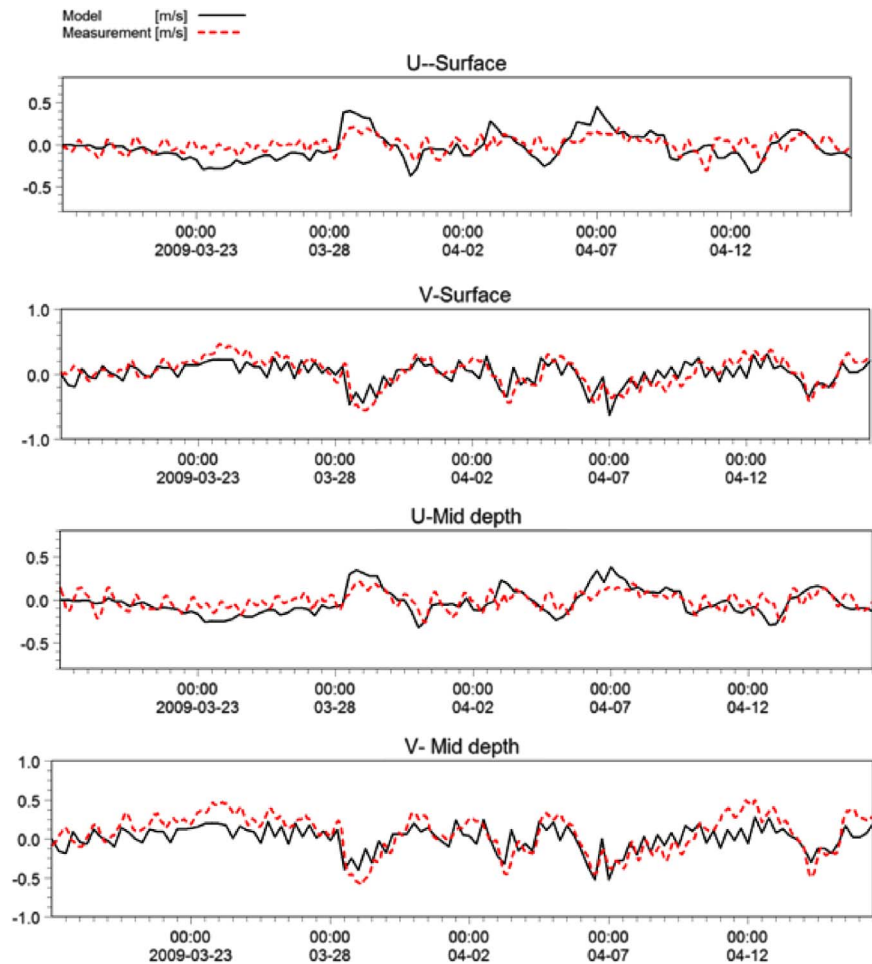


Fig. 10. Comparison of measured and simulated currents for CSI-3.

Table 1  
Willmott indices for different stations.

Station	U-surface	V-surface	U-Mid depth	V-Mid depth	Water level
CSI-3	0.66	0.71	0.75	0.62	–
Tiger Shoal	0.83	0.70	0.88	0.66	–
Trinity Shoal	0.92	0.83	0.94	0.83	0.83

Atchafalaya Bay, while current direction turned west in front of the Atchafalaya Bay, especially for areas surrounding Tiger and Trinity shoals. This change could be attributed to the complex bathymetry of the shoal environment, shallowness of the area, and also from the effect of fresh water plumes exiting the bay. Water level inside the Atchafalaya Bay increased by 0.2 m, while at Tiger and Trinity shoal area, water level set down as low as 0.1 m was observed. Westerly to northwesterly winds (Fig. 11b) produced eastward to southeastward flowing currents out of the bay (Fig. 12b). Similar to the southeasterly wind condition, the currents in the vicinity of the bay were affected by the local bathymetry and the river plumes discharged from the bay resulting a change in the current direction from eastward at north-western section of the bay to southeastward at Tiger and Trinity shoal complex and the southeastern sector. Incidentally, westerly to northwesterly winds with speed of about 10 m/s produced strong southerly and southeasterly currents (up to 0.5 m/s) offshore of the Trinity shoal. Similar persistent migration of river plumes from the Atchafalaya River towards ship shoal, located ~50 miles southeast of the bay were also previously reported (Kobashi, 2009).

Due to the peculiar alignment of the shoreline and the specific

location of the Atchafalaya Bay itself, water level would significantly decrease inside the bay (up to 0.6 m) during the passage of cold fronts in the winter-spring season. Cold fronts also have a significant effect on generating coastal currents in the bay area and the outer shelf. Although the northeasterly front (Fig. 11c; with a mean wind speed of about 7 m/s) and the corresponding current fields were not that strong compared to other selected events, currents from inside the bay to the outer shelf (Fig. 12c) could likely be associated with large scale transport of river sediments to the shelf area, including the Tiger and Trinity shoal complex. While the maximum current speed simulated for the mouth of the Atchafalaya Bay was about 0.25 m/s, for the outer shelf region it decreased to less than 0.05 m/s. Offshore of the Trinity shoal, current vectors veered toward northwest presumably as a result of intrusion of remote forcing propagated from the southern model boundary condition (notice that in front of the bay, current direction was southwestward which was consistent with the northeasterly wind direction, but over the outer shelf currents directed northwestward which could be due to the effect of boundary forcing). The effect of remote forcing on currents over the Louisiana shelf has also been reported by Chaichitehrani et al. (2014). Water level drop associated with this outer-shelf event was relatively large, showing a decrease of as much as 0.4 m for the Bay area and the outer shelf. However, for another cold front with northwesterly wind (speed of almost 13 m/s, Fig. 11d) intense currents were produced in the bay and the adjoining shelf area (Fig. 12d). At the peak of wind speed, general current direction over the shelf area was southeastward, while southward currents were produced inside the bay. A perceptible clockwise turn in current direction was evident in the post-frontal phase as well as an obvious increase in current speed, as indicated by current vectors



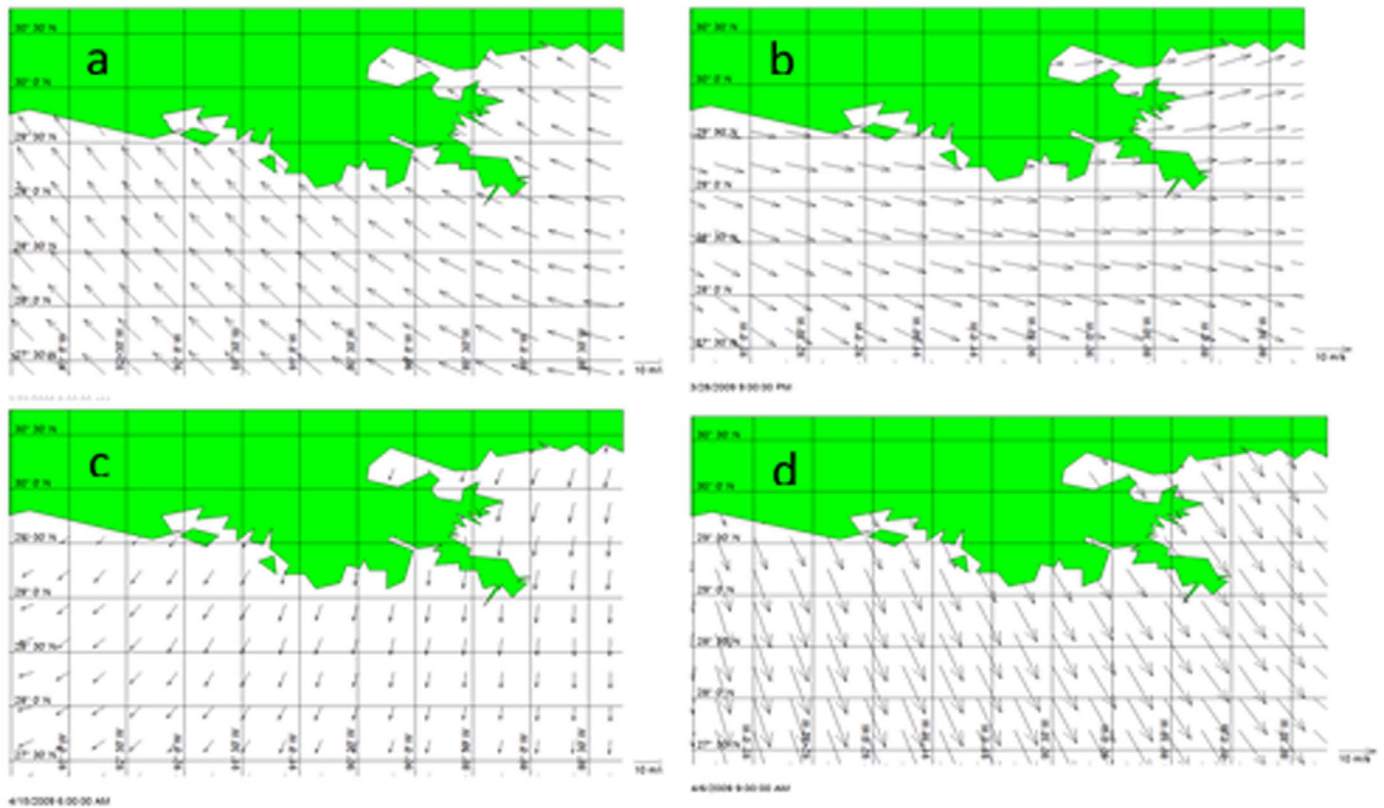


**Fig. 11.** Selected wind fields considered for the modeling case studies: a) southeasterly wind on 03/23/2009 at 9:00 AM, b) westerly to northwesterly wind on 03/28/2009 at 9:00 PM, c) northeasterly wind on 04/15/2009 at 6:00 AM, and d) northwesterly post-frontal phase of a cold front passage on 04/06/2009 at 9:00 AM.

approaching the Tiger and Trinity shoal complex (see Fig. 12d). Water level decreased over an extensive area inside and outside of the

Atchafalaya Bay, especially inside the bay, showing a drop as large as 0.8 m, and is consistent with an earlier study that reported substantial

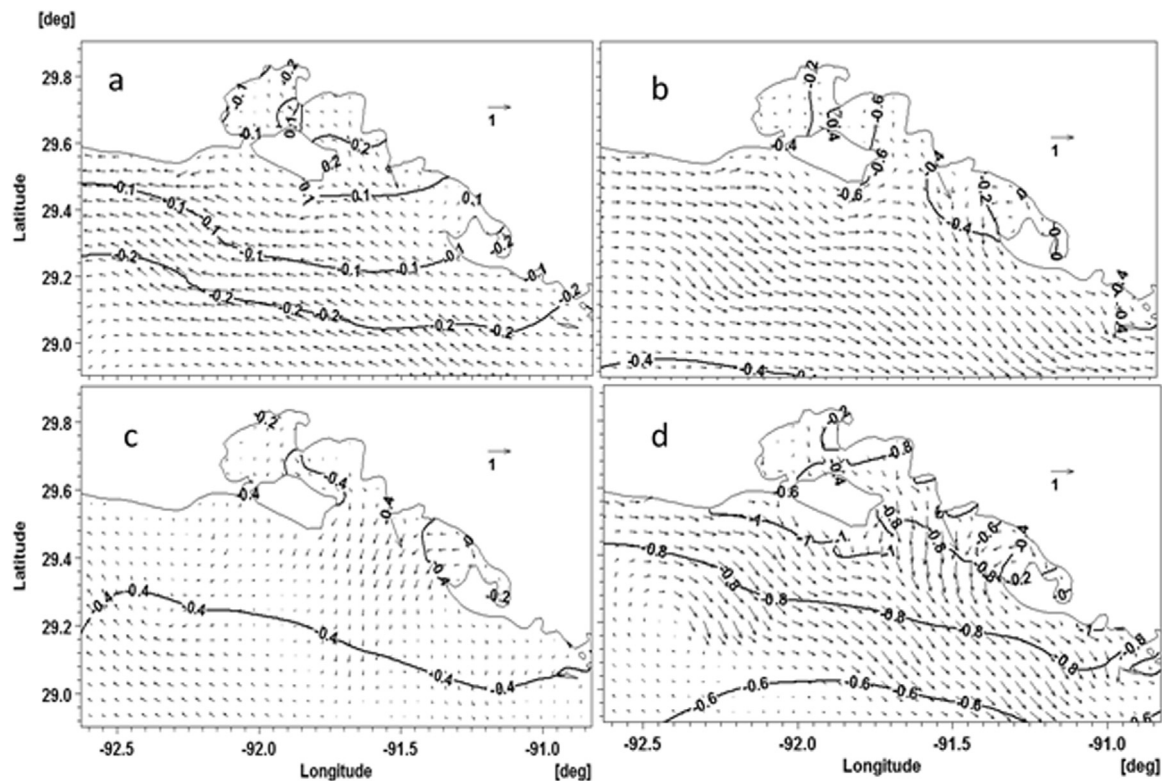


**Fig. 12.** Simulated current vectors (m/s) and water level (m) over the Atchafalaya Bay and the outer area for different time periods corresponding to, a) southeasterly wind, b) westerly to northwesterly wind, c) northeasterly wind, and d) northeasterly wind.

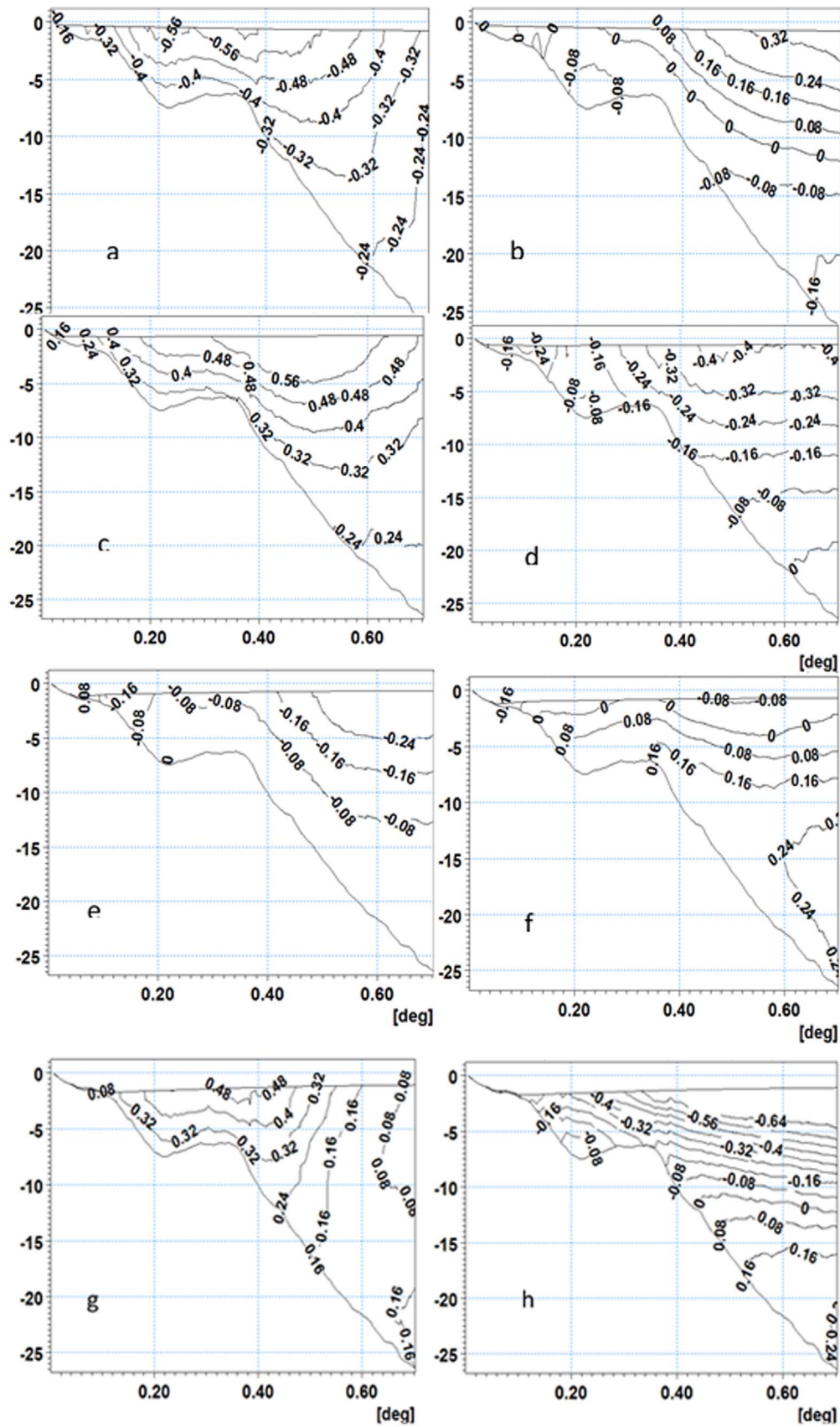


**Fig. 13.** (a) Variations of the simulated currents across transect 1 during different wind events, a, b) u and v component for southeasterly wind, c, d) u and v component for westerly to northwesterly wind, e, f) u and v component for northeasterly wind, and g, h) u and v component for northwesterly wind.

water level drop inside the Louisiana bays during cold front passages (Feng and Li, 2010).

## 5.2. Vertical current structure

Vertical coastal current structure and its dynamics during different wind events (Fig. 11) were analyzed by extracting vertical profiles of both east-west ( $u$ , positive eastwards) and north-south ( $v$ , positive shoreward) velocity components (Fig. 13) along an offshore transect extending from Marsh Island southward (Fig. 1). During the southeasterly wind event (Fig. 11a),  $u$  current component was significantly larger than the  $v$  component with current vectors directed westward throughout the entire water column (Fig. 13a, b). The  $u$  component of the flow at the surface off the Marsh island, where water depth was less than 10 m, was greater than 0.5 m/s; while the near-bottom current velocity was about 0.4 m/s. Similar strong current pattern near the shoal bed was reported from Ship Shoal, located off Atchafalaya Bay, corresponding to pre-frontal passages (Kobashi et al., 2007). Further offshore, current velocity decreased due to increasing water depth. For water depths shallower than 10 m, current velocity was weak and directed offshore accounting for the effect of wind. From the mid-section (depth 10 m) and up to the offshore end of the transect, currents were strong for the upper part of the water column (0.3 m/s) and directed shoreward. The contrasting direction of the cross-shore currents, between nearshore and offshore, demonstrates the effect of currents produced from the southern boundary influence, which included outer shelf variations and tidal forcing. Variations of  $u$ -component during the westerly-northwesterly wind event (Fig. 11b) were similar to the southeasterly wind (Fig. 13c, d). Velocity values were positive (eastward) and the maximum occurred at surface to mid-depth at a location having a total water depth of ~8 m. Corresponding  $v$ -component revealed offshore-directed currents for the entire water column along the transect (Fig. 13d). However, spatially varying slopes of current contours suggest the effect of offshore boundary in addition to the wind forcing. Intrusion of currents from the southern boundary was also noticeable within the current structure of both  $u$ - and  $v$ -components during northeasterly winds (Fig. 11c), when wind generated currents were not strong (Fig. 13e, f). Although wind induced offshore-directed currents dominated the surface layer along the cross-section, boundary forcing induced currents flowed shoreward across the major part of the water column (Fig. 13f). Direction of  $u$ -current component during a strong northwesterly wind event (Fig. 11d) was eastward for the entire water column with a maximum value of about 0.5 m/s near surface to a depth of almost 10 m of shelf waters (Fig. 13g). Offshore-directed current was dominant along the transect and velocity reached 0.64 m/s at 5 m below the surface, where water depth was as large as 25 m. The parallel orientation of the velocity contours suggested that the entire transect was affected by strong wind associated with the cold front passage. However, for water depth deeper than 15 m, the lower part of the water column was dominated by weak shoreward directed currents, presumably produced by the outer-shelf forcing from the southern boundary condition (Fig. 13h).

## 6. Discussion

### 6.1. Effect of currents on the Atchafalaya River plume

Fresh waters and fine sediments discharged from the Atchafalaya River into the Bay area can be transported to the shelf and further dispersed offshore under the influence of seasonally reversing coastal currents. The spatial variation of currents over the shelf south of the Atchafalaya Bay and corresponding wind directions, as obtained from numerical modeling, were presented in Section 5.1. The dominant current directions for each wind event are summarized in Table 2.

Circulation model outputs along with reliable data on the predominant wind direction during the peak of the Atchafalaya River

**Table 2**

Dominant direction of currents associated with different wind directions over the shelf south of the Atchafalaya Bay mouth.

Wind direction	Southeast	West-northwest	Northeast	Northwest
Current direction	West-northwest	Southeast	Southwest	South to Southeast

discharge can contribute to a better understanding of the fate of the mud plumes over the Atchafalaya shelf. Atchafalaya River discharge reaches the maximum during January–June with a peak that normally occurs in April (Allison et al., 2000; Roberts et al., 1980). Wind roses of measured wind data from CSI-3, encompassing the study duration (Fig. 14) indicate that for most of the time during late winter and spring (February, March, April, and May), wind blows from east to southeast, with high frequency of occurrence from southeast during the peak of discharge in April. It suggests that during this time, mud plume is strictly confined to the mouth of the Atchafalaya Bay and the coastline west of the bay (Murray, 1998). This observation is also consistent with the conclusion of Allison et al. (2000) about the existence of a flood induced mud deposit over the inner Atchafalaya shelf during the periods of high river discharge. They pointed out that the flood regime of the river, especially during March and April coincides with a significant decline in frequency and intensity of cold front passages. Available data on seabed transformation over the Atchafalaya shelf and modeling results from mud sediment transport reported from this coast also support this conclusion (Neill and Allison, 2005; Siadatmousavi et al., 2012; Jose et al., 2014). Seasonal field observation from the Tiger and Trinity Shoal complex (which is located farther south and beyond the influence of the established westward directed Atchafalaya mud plumes) suggested that accumulation of fine grained sediments at the shoal complex was minimal during the peak of the spring flood season (Jose et al., 2014). Instead, they reported a thick deposit of fine grained sediments, particularly from the Tiger shoal during December 2008, which was more likely transported by the southward currents induced by the frequent cold fronts during the winter time. The sustained westward transport of sediments during the peak flood season could also have contributed to the phenomenal growth of Chenier Plain west of the Atchafalaya Bay, with large scale accumulation of sediments originating from the Bay as mentioned by Huh et al. (2001) and Draut et al. (2005).

### 6.2. Lagrangian Tracking of coastal currents

To further study the effect of currents on the fate of suspended sediment load, especially the mud plumes originating inside and outside of the Atchafalaya Bay, model outputs were used to drive a Lagrangian particle tracking model. Under the effects of wind, river discharge, and outer-shelf variation, particle tracking simulation was performed on particles hypothetically released inside the bay and in the outer shelf (Fig. 15a; Lagrangian particle tracks shown as white lines). Inside the Bay, location of particle release was selected close to two outlets of the Atchafalaya River at Morgan City channel and Wax Lake Outlet. It can be seen that both particles moved towards the mouth of the bay and then were continuously transported westward to north-westward, almost parallel to the shoreline. The particles released outside of the bay, exhibited a continuous westward movement. Over the mid-shelf, the particle followed a northwestward track for ~50 km as a result of westward currents produced by southeasterly to southerly winds and then turned back and travelled ~100 km toward southeast. This eastward movement was produced by the frequent spreading of northerly winds during the post-frontal phase of the passing cold fronts combined with outer-shelf/tidal forcing from the southern boundary, as discussed in the previous section. The effect of southern boundary



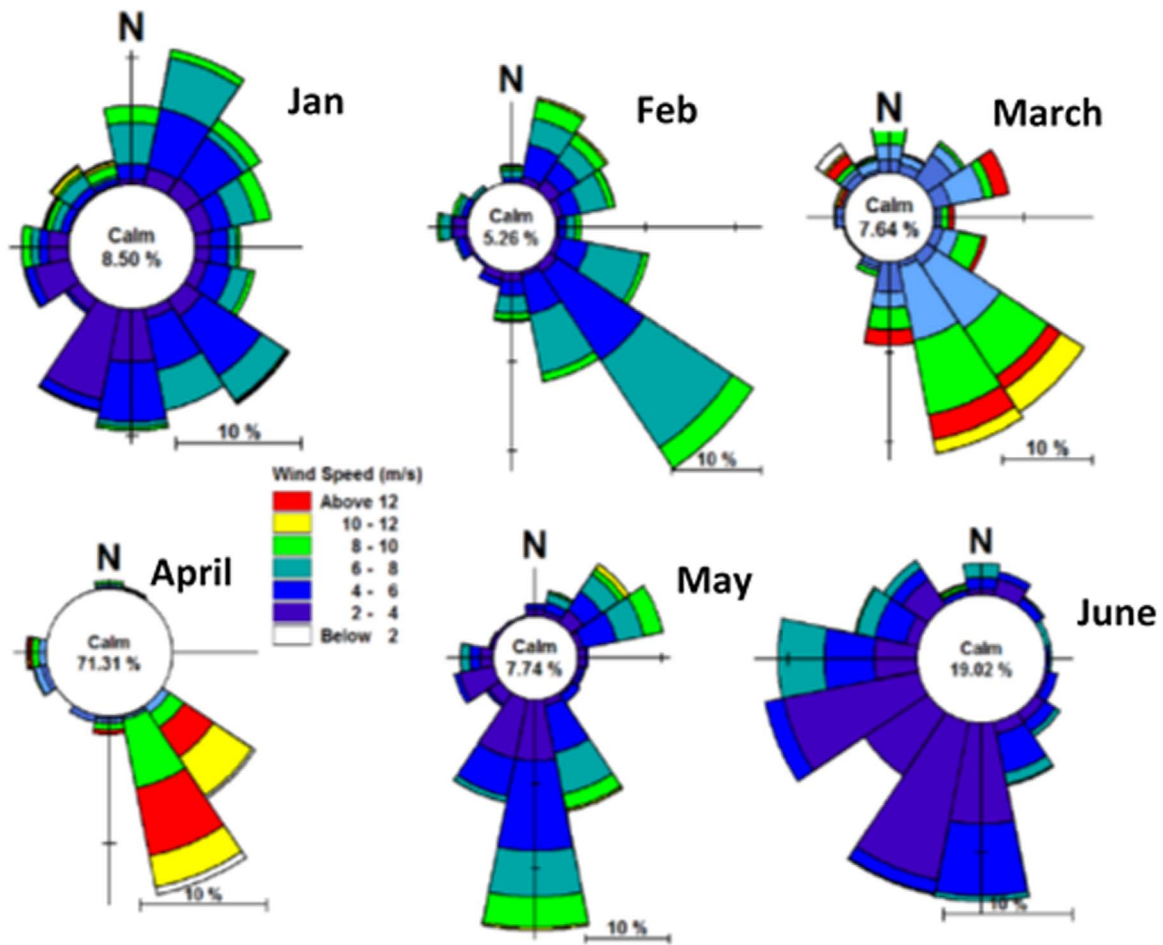


Fig. 14. Wind roses for January to June 2009 obtained from measured wind at CSI-3. Values in the circles represent the percentage of calm corresponding to wind speeds smaller than 2 m/s, Data courtesy WAVCIS/LSU.

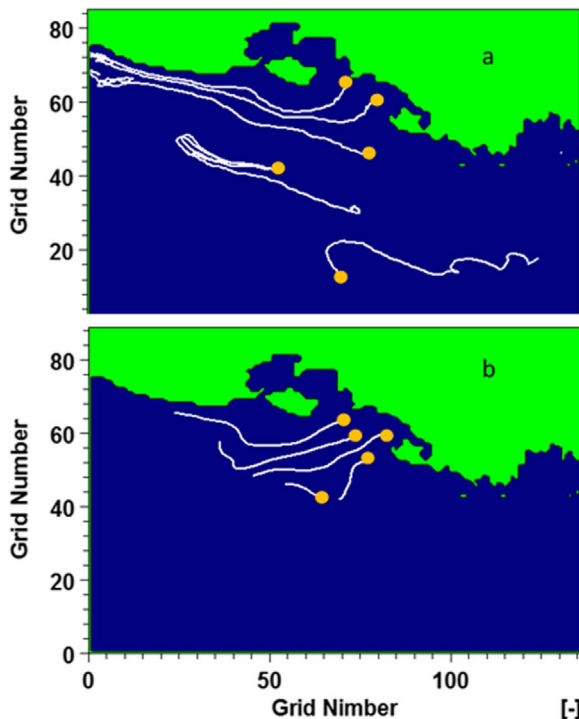


Fig. 15. Output from particle tracking using a Lagrangian modeling tool. a) Main simulation case that included all forcing, and b) simulation that included river discharge and excluding wind and outer-shelf boundary forcing.

on along-shelf transport was more pronounced, when the movement was tracked for a particle released at the outer shelf. For this location, the westward flow was negligible and the particle was almost continuously moved eastwards due to the dominance of outer-shelf eastward flow along the southern boundary. Flow tracking was also implemented for a modeling case considering only river discharge as the forcing. As for this case, shelf currents were negligible, and only particles released inside and in front of the Atchafalaya Bay were considered to examine the effect of river discharge on transport of suspended particles. All flow paths were limited to the mouth of the Bay (Fig. 15b). The river induced flow veered westward as a result of the Coriolis Effect (Kourafalou et al., 1996) and reached the Tiger and Trinity shoals at the end of the path and after that the flow was dissipated.

### 6.3. Current induced forcing: the effect of tides and outer-shelf variations

Allahdadi et al. (2013) showed a general agreement between the strength of prevailing wind and the coastal currents along the central Louisiana continental shelf and concluded that a substantial decline of wind stress during the summer is followed by weakening of currents. These results, however, do not include shallow coastal areas, particularly the Tiger and Trinity shoal complex. Over the shoaling complex and the adjoining shelf, moderate wind energy distributed across a shallower water column can produce strong currents. Therefore, it is imperative to examine the effect of other current generation forces including the combination of tide and outer-shelf phenomena on the circulation of the study area in addition to wind.

Simulation results presented in section 5–2 demonstrate substantial effect of wind on currents over the inner Atchafalaya shelf. In order to quantify this contribution, simulated currents from two different scenarios, and from different locations including Tiger shoal, Trinity shoal, and CSI-3 were compared. The scenarios include simulation with only wind forcing and simulation by inclusion of both wind and boundary forcing from coastal model. As illustrated in Section 4.3, simulations including both wind and boundary forcing resulted in much better agreement with measured data. The correlation of measured and simulated  $u$  and  $v$  current components for different stations show similar trends. For all stations, over 92% of the current variance (based on the correlation coefficient of the matchup comparison) for the  $u$  component could be explained by wind alone. For  $v$ -component, this contribution is smaller (between 82–86%) which is consistent with the sensitivity results provided in Section 4.1. The effects of outer-shelf phenomena and the tides are more pronounced in this direction and the variance in  $v$ -component is dominated by these forcings.

## 7. Summary and conclusion

Circulation dynamics of the Atchafalaya Bay and the inner Atchafalaya shelf under different wind conditions, outer-shelf variations/tide, and river discharge were studied using a well calibrated and skilled assessed 3-D circulation model. Simulated currents over the inner Atchafalaya shelf were sensitive to the outer-shelf boundary conditions, which includes forcing from both the impinging eddies shed from the Loop Current and the tides. Furthermore, the rate of wind energy transfer from the sea surface across the water column controlled by the vertical eddy viscosity parameter significantly affected simulated currents. Hence, the best matchup comparisons with measurements were obtained by including boundary forcing and the tuning of the vertical eddy viscosity. Shelf circulation off the Atchafalaya Bay was examined for different wind directions. The westward to north-westward currents produced by the predominantly southerly to northeasterly winds during the months of peak river discharge can profoundly influence the transport of river sediments to the Chenier plains located west of the Atchafalaya Bay. The westward transport of the river plume is not limited to the aforementioned wind conditions. Model results showed that, in the case of weakening of the wind, the plume will be deflected westward under the effect of the Coriolis force. The study was focused on the circulation and the coastal current variability under the influence of wind and outer-shelf forcing. However, the skill-assessed hydrodynamics model can be further used for quantifying transport and diffusion of mud plumes along the coastal Louisiana. The phenomenal growth of Chenier Plain west of the study area can be further investigated using this numerical model.

## Acknowledgments

The authors acknowledge partial support provided by a previous NASA grant (NNA07CN12A). DHI Water and Environment is acknowledged for providing an academic license for MIKE 3 modeling suite. In situ data from Tiger and Trinity Shoal complex were collected during a previous project funded by Bureau of Ocean Energy Management contract #M08AR12689, Department of Interior. Dr. Chunyan Li, Director of WAVCIS Lab is graciously acknowledged for providing the data from CSI-3 station.

## References

Allahdadi, M.N., Jose, F., Patin, C., 2013. Seasonal hydrodynamics along the Louisiana coast: implications for hypoxia spreading. *J. Coast. Res.* 29 (5), 1092–1100.

Allahdadi, M.N., Jose, F., Stone, G.W., D'Sa, E.J., 2011. The Fate of sediment plumes discharged from the Mississippi and Atchafalaya Rivers: An integrated observation and modeling study for the Louisiana shelf. In: *Proceedings, Coastal Sediments'11*, Miami, Florida, USA.

Allison, M.A., Kineke, G.C., Gordon, E.S., Goni, M.A., 2000. Development and reworking of a seasonal flood deposit on the inner continental shelf off the Atchafalaya River. *Cont. Shelf Res.* 20, 2267–2294.

Barron, C.N., Kara, A.B., Martin, P.J., Rhodes, R.C., Smedstad, L.F., 2006. Formulation, implementation and examination of vertical coordinate choices in the Global Navy Coastal Ocean Model (NCOM). *Ocean Model.* 11, 347–375.

Chaichitehrani, N., D'Sa, E.J., Ko, D.S., Walker, N.D., Osburn, C.L., Chen, R.F., 2014. Colored dissolved organic matter dynamics in the northern gulf of mexico from ocean color and numerical model results. *J. Coast. Res.* 30 (4), 800–814.

Cobb, M., Keen, T.R., Walker, N.D., 2008a. Modeling the circulation of the Atchafalaya Bay system during winter cold front events. Part 1: model description and validation. *J. Coast. Res.* 24 (4), 1036–1047.

Cobb, M., Keen, T.R., Walker, N.D., 2008b. Modeling the circulation of the Atchafalaya Bay system, part 2: River plume dynamics during cold fronts. *J. Coast. Res.* 24 (4), 1048–1062.

Cochrane, J.D., Kelley, F.J., 1986. Low-frequency circulation on the Chenier Plain coast on the Texas-Louisiana continental shelf. *J. Geophys. Res.* 91, 10,645–10,659.

Csanady, G.T., 1972. Response of large stratified lakes to wind. *J. Phys. Oceanogr.* 2, (3–13).

D'Sa, E.J., Ko, D.S., 2008. Short-term influences on suspended particulate matter distribution in the northern Gulf of Mexico: Satellite and model observations. *Sensors* 8, 4249–4264.

D'Sa, E.J., Roberts, H.H., Allahdadi, M.N., 2011. Suspended particulate matter dynamics along the Louisiana-Texas coast from satellite observation. In: *Proceedings, Coastal Sediments'11*, Miami, Florida.

DHI Water and environment, 2014. Mike 21 Flow model – FM, User Manual.

Draut, A.E., Kineke, G.C., Huh, O.K., Grymes, J.M., III, Westphal, K.A., Moeller, C.C., 2005. Coastal mudflat accretion under energetic conditions, Louisiana chenier-plain coast, USA. *Mar. Geol.* 214, 27–47.

Feng, Z., Li, C., 2010. Cold-front-induced flushing of the Louisiana Bays. *J. Mar. Syst.* 82, 252–264.

Huh, O.K., Walker, N.D., Moeller, C., 2001. Sedimentation along the Eastern Chenier Plain coast: down drift impact of a delta complex shift. *J. Coast. Res.* 17, 72–81.

Jose, F., Stone, G.W., 2006. Forecast of nearshore wave parameters using MIKE-21 spectral wave model. *Trans. Gulf Coast Assoc. Geol. Soc.* 56, 323–327.

Jose, F., Condrey, R.E., Fleeger, J.W., Liu, B., Gelpi, C., Siadatmousavi, S.M., Grippo, M., Kobashi, D., Dubois, S.F., 2014. Environmental Investigation of the Long-term use of Trinity and Tiger Shoals as Sand Resources for Large-scale Beach and Coastal Restoration in Louisiana, Final Report Submitted for Publication to BOEM, Department of Interior, p. 258.

Ko, D.S., Wang, D.-P., 2014. Intra-Americas Sea Nowcast/Forecast system ocean reanalysis to support improvement of oil-spill risk analysis in the Gulf of Mexico by multi-model approach, department of the interior, bureau of ocean. Energy Manag. Herndon BOEM 2014–1003, 55, <http://www.data.boem.gov/PI/PDFImages/ESPIS/5/5447.pdf>.

Ko, D.S., Preller, R.H., Martin, P.J., 2003. An experimental real-time Intra-Americas Sea Ocean Nowcast/Forecast System for coastal prediction. In: *Proceedings of the AMS 5th Conference on Coastal Atmospheric and Oceanic Prediction and Processes*, pp. 97–100.

Kobashi, 2009. Bottom Boundary Layer Physics and Sediment Transport along a Transgressive Sand Body, Ship Shoal, South-Central Louisiana: Implications for Fluvial Sediments and Winter Storms, unpublished (Ph.D. Dissertation), Louisiana State University.

Kobashi, D., Jose, F., Stone, G.W., 2007. Impacts of river discharges and winter storms on a sand shoal heterogeneous sedimentary environment, off south-central Louisiana, USA. *J. Coast. Res.* 50, 858–862.

Kourafalou, V.H., Oey, L.-Y., Wang, J.D., Lee, T.D., 1996. The fate of river discharge on the continental shelf: 1. Modeling the river plume and the inner shelf coastal current. *J. Geophys. Res.* 101 (C2), 3415.

Li, Y., Nowlin, W.D., Jr, Reid, R.O., 1997. Mean hydrographic fields and their inter-annual variability over the Texas-Louisiana continental shelf in spring, summer and fall. *J. Geophys. Res.* 102 (C1), 1027–1049.

Martin, P.J., 2000. A description of the Navy Coastal Ocean Model Version 1.0. Stennis Space Center, Mississippi: Naval Research Laboratory, NRL Report NRL/FR/7322–009962, p. 39.

Mossa, J., Roberts, H.H., 1990. Synergism of riverine and winter storm-related sediment transport processes in Louisiana's coastal wetlands. *Transactions. Gulf Coast Assoc. Geol. Soc.* 40, 635–642.

Murray, S.P., 1998. An Observational Study of the Mississippi-Atchafalaya Coastal Plume, *Technical Report*, US Department of the Interior, OCS Study MMS 98-0040, New Orleans, pp 516. ([www.data.boem.gov/PI/PDFImages/ESPIS/3/3238.pdf](http://www.data.boem.gov/PI/PDFImages/ESPIS/3/3238.pdf)).

Neill, C.F., Allison, M.A., 2005. Subaqueous deltaic formation on the Atchafalaya shelf, Louisiana. *Mar. Geol.* 214, 411–430.

Oey, L.Y., 1995. Eddy-forced and wind-forced shelf circulation. *J. Geophys. Res.* 100 (C5), 8621–8637.

Park, K., Kuo, A.Y., 1996. Effect of variation in vertical mixing on residual circulation in narrow, weakly nonlinear estuaries. In: *Friedrichs, C.T. (Ed.), Buoyancy Effects on Coastal and Estuarine Dynamics*, D.G. Aubrey and. American Geophysical Union, 301–317.

Rego, J.L., Meselhe, E., Stronach, J., Habib, E., 2008. Numerical modeling of the Mississippi-Atchafalaya rivers' sediment transport and fate: considerations for diversion scenarios. *J. Coast. Res.* 26, 212–229.

Roberts, H.H., Sneider, J., 2000. Atchafalaya Basin and Atchafalaya-Wax lake deltas – the new regressive phase of the Mississippi River Delta complex. *Am. Assoc. Pet. Geol. Field Guideb.*, 68.

Roberts, H.H., Adams, R.D., Cunningham, R.H.W., 1980. Evolution of sand-dominant

- subaerial phase, Atchafalaya Delta, Louisiana. *Am. Assoc. Pet. Geol. Bull.* 64, 264–279.
- Roberts, H.H., Braud, D., Edrington, C., Khalil, S.M., 2010. Results of a Geophysical and Sedimentological Evaluation: tiger-trinity Shoals as Sources of Sand for Coastal Restoration. *Coast. Stud. Inst. State Univ.*, 45, (p).
- Saenko, O.A., 2006. The effect of localized mixing on the ocean circulation and time-dependent climate change. *J. Phys. Oceanogr.* 36, 140–160.
- Sheremet, A., Stone, G.W., 2003. Observations of nearshore wave dissipation over muddy sea beds. *J. Geophys. Res. Oceans* 108, 3357.
- Sheremet, A., Mehta, A.J., Liu, B., Stone, G.W., 2005. Wave–sediment interaction on a muddy inner shelf during Hurricane Claudette. *Estuar., Coast. Shelf Sci.* 63, 225–233.
- Siadatmousavi, S.M., Jose, F., Chen, Q., Roberts, H.H., 2013. Comparison between optical and acoustical estimation of suspended sediment concentration: field study from a muddy coast. *Ocean Eng.* 72, 11–24.
- Siadatmousavi, S.M., Allahdadi, M.N., Chen, Q., Jose, F., Roberts, H.H., 2012. Simulation of wave damping during a cold front over the muddy Atchafalaya shelf. *Cont. Shelf Res.* 47, 165–177.
- Stone, G.W., Jose, F., Luo, Y., Siadatmousavi, S.M., Gibson, W.J., 2009. A WAVCIS-based ocean observing station off Eglin Air Force Base, Fort Walton, Florida. In: *Proceeding of OCEANS 2009 MTS/IEEE (Biloxi, Mississippi, Marine Technology Society and IEEE)*, pp. 1–9.
- Tehrani, N.C., D'Sa, E.J., Osburn, C.L., Bianchi, T.S., Schaeffer, B.A., 2013. Chromophoric Dissolved Organic Matter and Dissolved Organic Carbon from Sea-Viewing Wide Field-of-View Sensor (SeaWiFS), Moderate Resolution Imaging Spectro-radiometer (MODIS) and MERIS. *Sens.: Case Study North. Gulf Mex. Remote Sens.* 5 (3), 1439–1464.
- Walker, N.D., Hammack, A.B., 2000. Impacts of winter storms on circulation and sediment Transport: atchafalaya-vermilion Bay Region, Louisiana, USA. *J. Coast. Res.* 16, 996–1010.
- Willmott, C.J., 1981. On the validation of models. *Phys. Geogr.* 2, 184–194.
- Wright, L.D., Sherwood, C.R., Sternberg, R.W., 1997. Field measurements of fair weather bottom boundary layer processes and sediment suspension on the Louisiana inner continental shelf. *Mar. Geol.* 140, 329–345.
- Zhang, J.L., Steele, M., 2007. Effect of vertical mixing on the Atlantic Water layer circulation in the Arctic Ocean. *J. Geophys. Res. Oceans* 112, 1–9.
- Zhang, X.P., 2003. Design and Implementation of an Ocean Observing System: Wavcis (Wave-Current-Surge Information System) and Its Application to the Louisiana Coast. Louisiana State University, Baton Rouge, Louisiana, 182.